International Journal of Immunopathology & Pharmacology

Original Research Article

Effect of Chinese herbal compound GAPT on the early brain glucose metabolism of APP/PS1 transgenic mice

International Journal of Immunopathology and Pharmacology
Volume 33: 1–13

DOI: 10.1177/2058738419841482
journals.sagepub.com/home/iji
SAGE

Lulu Mana[1,2], Huili Feng[1,3], Yunfang Dong[1,4], Yahan Wang[1,2], Jing Shi[1,5], Jinzhou Tian[1,5] and Pengwen Wang[1,2]

Abstract

A number of studies have shown that early-stage Alzheimer's disease (AD) is associated with abnormal brain glucose metabolism before cognitive decline, which may be the key pathological change of asymptomatic AD. The pathogenesis of AD in traditional Chinese medicine is kidney deficiency and turbid phlegm. Based on this, GAPT (a mixture of herbal extracts) was made to invigorate kidney Yang and eliminate phlegm. Previous studies have shown that GAPT can improve and delay the memory decline, but the specific therapeutic target of AD in an early stage has not been studied. The aim of this study was to investigate the effect of GAPT on glucose metabolism in the early stage of AD. Eighty-eight 3-month-old male APP/PS1 transgenic mice were randomly divided into model group; donepezil group; and low, middle and high GAPT dosage groups. Twelve 3-month-old C57BL/6J mice were used as a control group. The Morris water maze test and the Step-Down Passive-Avoidance test were used to evaluate learning and memory ability. Cerebral extraction and the accumulation of glucose were scanned with a micro-positron-emission tomography (PET) imaging system. Immunohistochemistry, western blot analysis and polymerase chain reaction (PCR) were used to detect the expression of the PI3K/AKT-mTOR signalling pathway–related proteins and messenger RNAs (mRNAs) in hippocampus of APP/PS1 transgenic mice after 3 months of drug administration. GAPT can shorten the escape latency and error numbers compared to the model group. In micro-PET imaging analysis, GAPT can increase the glucose uptake average rate in the frontal lobe, temporal lobe, parietal lobe and hippocampus. The immunohistochemistry, western blot analysis and PCR results indicated that GAPT can increase the expression of PI3K, AKT, GLUT1 and GLUT3 in the hippocampus of APP/PS1 transgenic mice. In summary, GAPT can improve brain glucose metabolism damage in APP/PS1 transgenic mice, mainly by increasing brain glucose uptake, increasing glucose transport and improving the insulin signalling pathway.

Keywords

Alzheimer's disease, APP/PS1 transgenic mice, cerebral glucose metabolism, Chinese herbal compound GAPT, insulin signalling transduction

Date received: 12 November 2018; accepted: 7 March 2019

[1]Key Laboratory of Chinese Internal Medicine of Ministry of Education and Beijing, Dongzhimen Hospital, Beijing University of Chinese Medicine (BUCM), Beijing, China
[2]Key Laboratory of Pharmacology of Dongzhimen Hospital (BUCM), State Administration of Traditional Chinese Medicine, Beijing, China
[3]The First Hospital Affiliated to Henan University of Traditional Chinese Medicine, Zhengzhou, China
[4]Zhongkang International Health Physical Examination Center, Qingdao Ruiyuan Hospital of Traditional Chinese Medicine, Qingdao, China
[5]Beijing University of Chinese Medicine, BUCM Neurology Center, Dongzhimen Hospital, Beijing, China

Corresponding author:
Pengwen Wang, Key Laboratory of Chinese Internal Medicine of Ministry of Education and Beijing, Dongzhimen Hospital, Beijing University of Chinese Medicine (BUCM), No. 5 Haiyuncang, Dongcheng District, Beijing 100700, China.
Email: pw_wang@163.com

Alzheimer's disease (AD) is thought to be one kind of chronic progressive neurodegenerative disease that is prevalent with age. The prominent feature of AD is the deterioration of recent memory, cognition and physical status. The irreversible process of AD is characterized by certain specific neuropathological hallmarks, such as neuronal loss, accompanied by synaptic damage,[1] extracellular deposits of amyloid fibrils as amyloid plaques or senile plaques and intraneuronal neurofibrillary tangles (NFTs) of hyperphosphorylated tau.[2] The mechanisms underlying AD are quite complicated and remain uncertain. Over the past decade, a wealth of epidemiological evidence has suggested that AD should be regarded as a degenerative metabolic disease. Inadequate glucose metabolism associated with insulin/insulin-like growth factor (IGF) resistance and deficient energy utilization was observed in advance of clinically measurable cognitive decline.[3–6] It has also been reported that diabetic patients experience a higher incidence of AD than non-diabetic patients.[7] A decreased cerebral metabolic rate for glucose (CMRglc) in the hippocampus and posterior cingulate cortices[8] progressively leads to an insufficient brain energy supply that is responsible for the characteristic neuropathologic changes of AD. This illustrates the importance of cerebral glucose metabolism, which may be a critical pathologic change in the clinical asymptomatic stage of AD.

Cerebral glucose metabolism significantly depends on the function of glucose transportation.

Glucose transporters (GLUTs), especially GLUT1 and GLUT3, play an essential role in maintaining normal neurological functions[9] and glucose uptake of the brain.[10] Decreased GLUT1 activity has been recognized in the AD brain[11] along with insulin/IGF resistance.[12] Meanwhile, the phosphatidylinositol 3-kinase (PI3K)/protein kinase B (AKT)/mTOR signalling pathway and its major activators insulin and IGF-1 can effectively mediate neuronal responses to neurotransmission and metabolic control.[13] Previous studies have shown that insulin de-sensitization, downregulation of phosphorylated AKT and cognitive decline were recognized in a streptozotocin (STZ)-induced AD rat model.[14]

Currently, although agents targeting cholinergic transmission and glutamate release can slow cognitive decline, degenerative progression of AD could not be effectively reversed or halted. Traditional Chinese medicine (TCM) that acts on multiple targets of AD is being developed extensively. Patented Chinese herbal compound GAPT (also called GEPT or Jinsiwei) is a mixture of herbal extracts that includes Radix Ginseng, *Acorus gramineus* Soland, Radix Polygalae and Radix Curcuma (containing ingredient of turmeric). The pathogenesis of AD in TCM is kidney deficiency and turbid phlegm. Based on this, GAPT was made to invigorate kidney Yang and eliminate phlegm. The clinical practice of GAPT has shown remarkable effects, and previous studies concurrently proved that GAPT improved memory and cognitive functions of APPV7171 transgenic mice, increased synaptophysin (SYP) expression and protected synapses before and after the formation of amyloid plaques.[15] GAPT also decreased the level of GSK-3β expression in the brain cortex of AD rats.[16] However, its specific therapeutic targets in the early stages of AD are still unclear. Therefore, taking brain glucose metabolism in the early stage of AD as the appropriate entry point, we investigated the therapeutic effects of GAPT in APP/PS1 double transgenic mice and illustrated its possible therapeutic mechanism specifically related to insulin signalling, synapse ultrastructure and glucose metabolism.

Materials and methods

Drug preparation

GAPT, a combination of herbal extracts, provided by Dongzhimen Hospital (Beijing University of Chinese Medicine, Beijing, China), was dissolved in 0.5% carboxymethyl cellulose (CMC) at a concentration of 30 mg/mL. Hydrochloric acid donepezil tablets, which were provided by Eisai (China) Pharmaceutical Company Limited (Batch No: 140635), were crushed and dissolved in 0.5% CMC at a concentration of 0.092 mg/mL.

Animals and administration

Eighty-eight 3-month-old male APP/PS1 transgenic mice and 18 3-month-old male C57BL/6J littermate mice were provided by Beijing Huafukang Bioscience Company limited (SCXK(Beijing)2014-0004). All mice were kept in the Barrier Environment Animal Lab of the Key Laboratory of Pharmacology of Dongzhimen Hospital, affiliated with Beijing University of

Chinese Medicine. All animals were kept in a stable environment at 22°C with a 12-h light/dark cycle and they had free access to food and water. All experiments were performed in compliance with Beijing's regulations and guidelines for the use of animals in research, and the study was approved by the Animal Research Ethics Board of Dongzhimen Hospital.

Three-month-old male APP/PS1 transgenic mice were randomly divided into five groups and they received intragastrically administered vehicle or medicines. The APP group (n = 17) was given 0.5% CMC, the Donepezil group was given donepezil (APP + D, n = 18; 0.92 mg/kg/d i.g.), the GAPT groups were given a small dose (APP + Gs, n = 17; 5 g/kg/d i.g.), a middle dose (APP + Gm, n = 18; (10 g/kg/d i.g.) or a high dose (APP + Gh, n = 18; 20 g/kg/d i.g.) of GAPT for 3 months. Three-month-old male C57BL/6J mice were used as the control group (n = 18) and they were given 0.5% CMC for 3 months as well.

Morris water maze test

A Morris water maze (MWM) test was used to evaluate spatial memory function. This test was performed in a circular container (120 cm diameter, 40 cm height) containing opaque water (22°C ± 1°C). The pool was divided into four quadrants (quadrant I, II, III and IV) labelled with different external navigation marks. The MWM test lasted for five consecutive days. In the first day, mice were individually placed on a hidden fixed platform 2 cm beneath the water surface in quadrant III (target quadrant) for 10 s to memorize its location. The mice were given four trials per day by releasing them into the water from each of the remaining quadrants. In the 120-s process of locating the hidden platform per training trial, the escape latency and swimming route were recorded via the digital camera above the container. If the mouse failed to locate the platform within 60 s, the next trial was given by manually placing it back on the platform for 10 s. The hidden platform was removed on the fifth day of the test. All mice were placed in quadrant I and allowed to swim freely for 120 s. The distance and time spent to reach quadrant III was recorded and quantified (Shanghai Transfer Information Technology CO., LTD).

Step-Down Passive-Avoidance test

The Step-Down Passive-Avoidance (SDPA) test was used to appraise the learning and memory ability of animals by passively avoiding electrical stimulation. The bottom of the testing case had a stainless-steel grid floor, with a shock free zone (SFZ). All mice were given a certain amount of electrical stimulation (36 V) in the process of test. The experiment was divided into 2 days (training and testing). Day 1 was the acquisition trial in that mice were placed on the SFZ. By repeatedly giving electric shock when stepping down on the grid floor, mice were eventually trained to stay on the SFZ. After 24 h, performance of passive avoidance was tested. Each mouse was placed on the SFZ again, and the step-down latency (SDL) and number of stepping downs (the number of errors) were observed and quantified (Shanghai Transfer Information Technology CO., LTD).

Micro-positron-emission tomography imaging

Cerebral extraction and accumulation of glucose was scanned with a micro-positron-emission tomography (PET) imaging system (INVEON PET/CT, Siemens Healthcare, Erlangen, Germany). The system included 64 lutetium silicate crystals with a PET temporal resolution of less than 1.5 ns, a visual field length measured in the axial direction of 12.7 cm and an axial resolution of less than 1.7 mm from the centre of 1 cm. Attenuation correction was performed on image acquisition by CT, and the correction scanning was performed for approximately 5 min. Each of the mice was scanned for 10 min. Tracer material 18F-FDG was provided by the Tumor Hospital of the Chinese Academy of Medical Sciences, Beijing, China. Three mice were randomly selected per group and fasted for 6 h before the test. The mice were placed in a transparent box and completely anaesthetized by inhaling 2% isoflurane. Approximately 530–650 μCi radioactive tracer 18F-FDG was injected through the tail vein. Micro-PET images were collected at 1 h after the injection. Micro-PET image reconstruction was performed using the filtering projection algorithm and CT photon attenuation correction (0.2 mm × 0.2 mm × 0.8 mm). The whole brain three-dimensional (3D) region of interest (ROI) was manually selected in PET/CT images of the cross section, sagittal plane and coronal plane of

Table 1. The primer sequence.

Name	Forward	Reverse	Size (bp)
GAPDH	5′-TGCCCCCATGTTTGTGATG-3′	5′-TGTGGTCATGAGCCCTTCC-3′	151
PI3K	5′-TCCAAATACCAGCAGGATCA-3′	5′-ATGCTTCGATAGCCGTTCTT-3′	137
Akt	5′-GAACGGCCTCAGGATGTGGA-3′	5′-GGTGCGCTCAATGACTGTGG-3′	144

GAPDH: glyceraldehyde 3-phosphate dehydrogenase; PI3K: phosphatidylinositol 3-kinase.

the mice to calculate the percentage of dose per gram of brain tissue injected in the ROI (%ID/g).

Immunohistochemistry

Six mice were randomly selected for immunohistochemical staining in each group. Mice were anaesthetized with 4% chloral hydrate. The thoracic cavity was opened to expose the heart. The left ventricle apex was cut and a catheter was inserted. Then, the right atrial appendage was cut and the vessels were flushed rapidly with normal saline (NS) until the fluid was clear. Subsequently, perfusion with 4% paraformaldehyde was performed until the liver and limbs were pale and stiff. Fixed brain tissue was cut into 4 μm slices after the hippocampus was observed. Immunohistochemistry was performed as described previously.[17] The slices were heated at 56°C for 1 h and then dewaxed in dimethylbenzene and hydrated in alcohol (100%, 95%, 80% and 70%). The sections were soaked in 3% H_2O_2 for 15 min, and antigens were retrieved by citric acid buffer (pH 6.0) in a microwave for 5 min. Tissues were incubated with primary antibodies (AKT, 1:1000, Abcam, USA; Glut1, 1:250, Abcam, USA) in humidified boxes at 4°C overnight. On the following day, the slices were incubated with biotin-conjugated secondary antibodies (ZSGQ-BIO, Beijing, China). The expression of Akt and Glut1 proteins in the hippocampal CA1 area was detected by DAB (ZSGQ-BIO, Beijing, China). To verify the specificity of antibodies, goat serum was used as the negative control instead of primary antibodies in each test. The number of positively stained neurons in the CA1 area of the hippocampus were observed and counted at ×20 magnification. All images were captured with Motic Med 6.0 Image software.

Western blot

Mice were anaesthetized with 4% chloral hydrate and euthanized by cervical dislocation. Immediately stripped brain tissue was placed on ice and the cortex and hippocampus were separated. The concentration of hippocampal proteins was measured with bicinchoninic acid (BCA). An equal amount of total protein was separated with SDS-PAGE and transferred to polyvinylidene fluoride (PVDF) membranes. The proteins were blocked with 5% skimmed milk and subsequently incubated in a primary antibody to PI3Kp85 (1:1000, CST, USA), Akt (1:1000, Abcam, USA), p-MTOR (1:1000, CST, USA), p-GSK3β (1:1000, CST, USA), Glut1(1:500, Abcam, USA), Glut3 (1:8000, Abcam, USA) and β-actin (1:8000, Abcam, USA) at 4°C overnight. After washing with PBST three times, proteins were incubated with the secondary antibody (1:8000, ZSGQ-BIO, Beijing, China) for an hour at room temperature. ECL was performed for visualization. The results were analysed with ImageJ software.

Gene expression assessment

Protocols for total RNA extraction, complementary DNA (cDNA) synthesis and quantitative real-time polymerase chain reaction (PCR) were described previously.[18] Tissues of the hippocampus were extracted for total RNA with a Trizol kit (Invitrogen, Carlsbad, CA, USA). According to M-mlv reverse transcription kit (Takara, Shiga, Japan) instructions, total RNA was synthesized to cDNA. Real-time PCR was performed with FastStart Universal SYBR Green Master (Rox) (Roche, Switzerland) and monitored with a real-time PCR system (Applied Biosystems 7500 Real-Time PCR Systems). The primer sequences are summarized in Table 1. The relative expression levels of each primer sequence messenger RNA (mRNA) were analysed by the $2^{-\Delta\Delta Ct}$ algorithm, normalized to glyceraldehyde 3-phosphate dehydrogenase (GAPDH) and relative to the control groups.

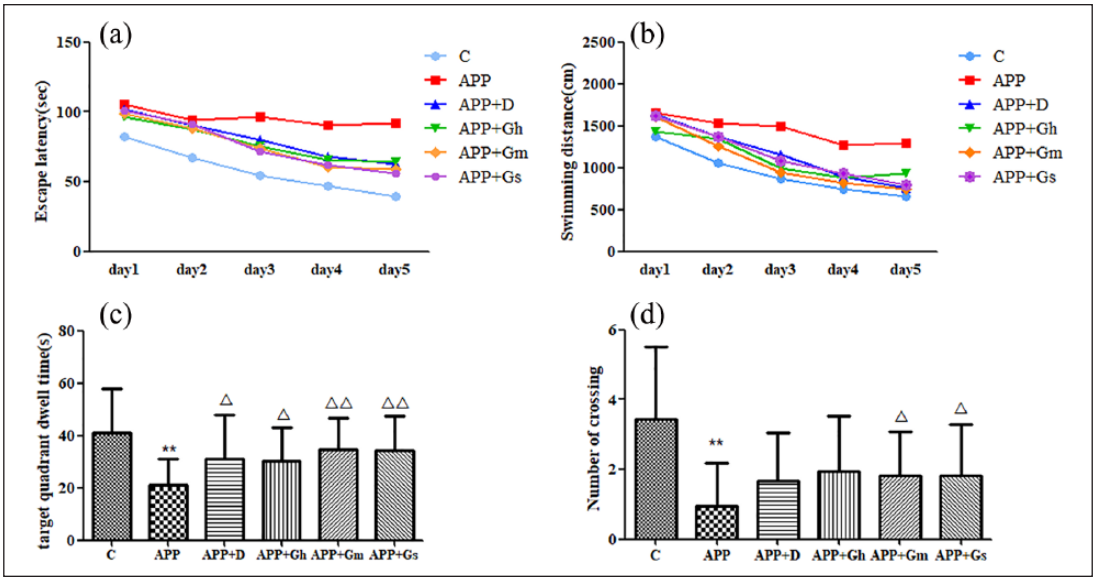

Figure 1. Effect of GAPT on (a) escape latency, (b) swimming distances, (c) target quadrant dwelling time and (d) number of APP/PS1 transgenic mice crossing the platform in the MWM test. Control: C57BL/6J mice; APP: APP/PS1 mice; APP + D: donepezil; APP + Gs: GAPT small dose; APP + Gm: GAPT middle dose; APP + Gh: GAPT high dose.
**$P < 0.01$ versus control group, △$P < 0.05$ versus model group and △△$P < 0.01$ versus model group; ANOVA. Each group showed a decreasing trend with the increase in training times. The escape latency and swimming distances of the control group were significantly decreased from the first day compared to those of the model group ($P < 0.01$). On the fourth day and fifth day, the escape latencies of all intervention groups were shortened ($P < 0.05$). The target quadrant dwelling time of each intervention group was increased compared with the model group ($P < 0.05$). The GAPT middle and small dose groups crossed the target platform obviously more frequently than the model group ($P < 0.05$).

Results

Effects of GAPT on spatial learning and memory deficits in APP/PS1 transgenic mice

MWM test. MWM test was used to evaluate learning and memory functions. As shown in Figure 1, during the 5-day positioning navigation task and spatial probe test, the escape latency of the control group was significantly shortened compared with the APP/PS1 transgenic mice group (model group) from the first day ($P < 0.01$). In the third day of the test, the escape latency of the GAPT small-dose group was shortened compared with the model group ($P < 0.05$), and from the fourth day, the escape latencies of all intervention groups were remarkably shortened ($P < 0.05$; Figure 1(a)). Meanwhile, the running distances of each group to find the platform were decreased with the training. Compared with the model group, the running distance of the control group was reduced from the first day. The distance of each intervention group was significantly decreased from the fourth day ($P < 0.01$ or $P < 0.05$; Figure 1(b)).

The APP/PS1 transgenic mice crossed the target quadrants less frequently and spent less time on the target platform compared with the control group ($P < 0.01$). The target quadrant dwelling time of each intervention group was increased compared with that of the model group ($P < 0.05$; Figure 1(c)), while the GAPT middle-dose group and GAPT small-dose group obviously crossed the target platform more frequently than the model group ($P < 0.05$; Figure 1(d)).

SDPA test. As shown in Figure 2, compared with the model group, 24 h after training, the error number of the control group was significantly decreased ($P < 0.01$). The error number of the donepezil group and GAPT middle-dose group was decreased ($P < 0.05$), and the error number of the GAPT small-dose group was obviously decreased ($P < 0.01$) compared with that of the model group (Figure 2(a)). At the later stage of training, the latency of the model group was significantly shorter than that of the normal group ($P < 0.01$), while there was no difference between the donepezil group and the model group ($P > 0.05$). The latency of each GAPT group was prolonged or significantly prolonged compared with that of the model group ($P < 0.01$ or $P < 0.05$) (Figure 2(b)).

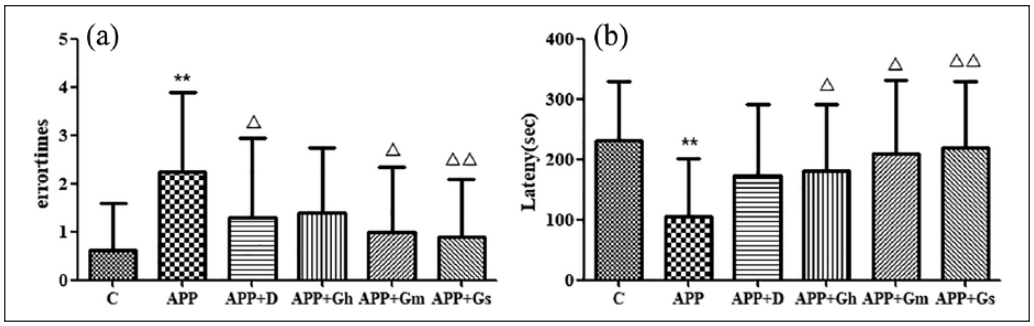

Figure 2. Effect of GAPT on (a) error time and (b) latency in APP/PS1 transgenic mice in the SDPA test. Control: C57BL/6J mice; APP: APP/PS1 mice; APP + D: donepezil; APP + Gs: GAPT small dose; APP + Gm: GAPT middle dose; APP + Gh: GAPT high dose. $^{**}P < 0.01$ versus control group, $\triangle P < 0.05$ versus model group, $\triangle\triangle P < 0.01$ versus model group; ANOVA. Compared with the model group, the number of errors was significantly reduced in the control group after training ($P < 0.01$). The number of errors was reduced in the donepezil group and GAPT middle dose group ($P < 0.05$), while the number of errors was significantly reduced in the GAPT small dose group ($P < 0.01$) compared with the model group.

Effects of GAPT on the cerebral extraction and accumulation of glucose on APP/PS1 transgenic mice. In Figure 3(a), the brain micro-PET images of different groups were intuitively observed. The extraction and accumulation of glucose in the ROI (frontal lobe, temporal lobe, parietal lobe and hippocampus) were reduced in the APP/PS1 transgenic mice compared with the control group. In the donepezil group and GAPT middle- and small-dose groups, extraction and accumulation of glucose in the ROI were increased compared with the model group (Figure 3(b)).

The cerebral glucose uptake rates in the ROIs were quantitatively analysed. The APP/PS1 transgenic mice showed a trend towards the glucose uptake average rate in the ROIs compared to the normal control group. Compared with the model group, the glucose uptake average rates in the ROIs were increased in the donepezil group and GAPT middle- and small-dose groups (Figure 3(b)).

Effects of GAPT on PI3K, AKT, p-GSK3β and p-mTOR expression levels in APP/PS1 transgenic mice. Western blot analysis showed a significant decrease in PI3K in the hippocampus of APP/PS1 transgenic mice compared to the control group ($P < 0.05$). PI3K expressions in the donepezil- and GAPT-treated groups were all increased ($P < 0.05$), and there was a significant difference between the GAPT middle-dose group and the model group ($P < 0.01$; Figure 4(a)).

Immunohistochemical staining showed positive brownish-yellow coloured particles in the hippocampal CA1 region of APP/PS1 transgenic mice. The expression of Akt in the hippocampal CA1 region in APP/PS1 transgenic mice was significantly reduced compared with the control group ($P < 0.01$). Compared with the model group, the expression of Akt was significantly increased in each treatment group ($P < 0.05$ or $P < 0.01$; Figure 5(a)). Western blot analysis showed a basically similar Akt expression pattern as immunohistochemistry analysis showed in each group. The expression of Akt was significantly reduced in the model group compared with the normal group, while it was significantly increased in the donepezil and GAPT middle-dose group ($P < 0.01$). The expression of Akt was similarly increased in the GAPT high-dose group ($P < 0.05$; Figure 5(b)).

Western blot analysis showed a significant decrease in p-GSK3β in the hippocampus of APP/PS1 transgenic mice compared to that in the control group ($P < 0.01$). Compared with the model group, the expression of p-GSK3β in the donepezil group and GAPT high- and small-dose groups were increased ($P < 0.05$), while the expression of p-GSK3β in the GAPT middle-dose group was significantly increased ($P < 0.01$; Figure 6(a)). Meanwhile, western blot analysis showed a significant increase in p-mTOR in the hippocampus of APP/PS1 transgenic mice compared to that in the control group ($P < 0.01$). Compared with the model group, the expression of p-mTOR in the donepezil group was decreased ($P < 0.05$), while the expression of p-mTOR in the GAPT high- and middle-dose groups were significantly decreased ($P < 0.01$; Figure 6(b)).

Effects of GAPT on PI3K mRNA and AKT mRNA expression levels in APP/PS1 transgenic mice. The relative concentrations of the PI3K and Akt genes and the internal reference GAPDH gene expression were obtained

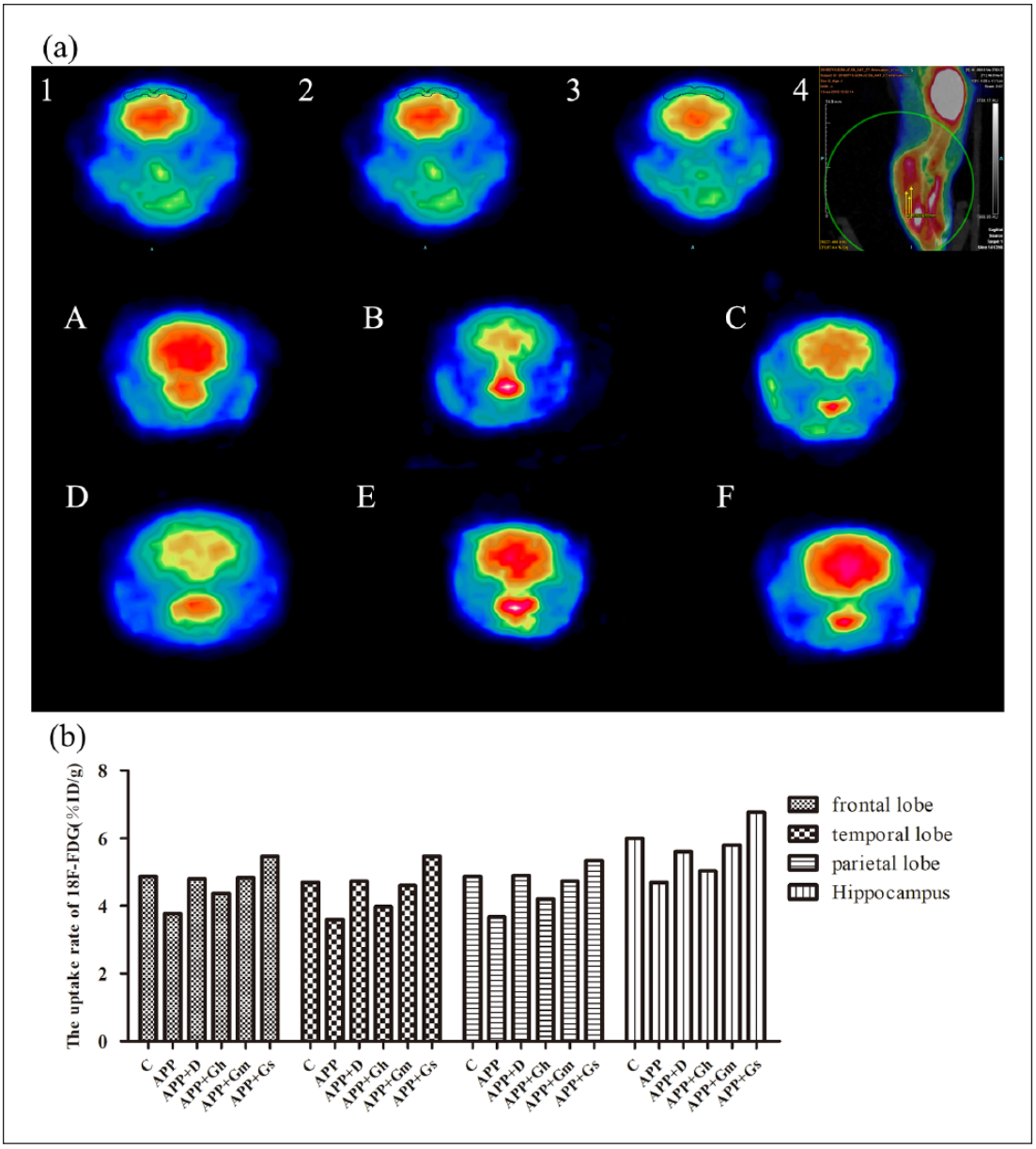

Figure 3. (a) The brain micro-PET images of different groups and (b) cerebral glucose uptake rates in the ROIs were intuitively observed. 1: IOC of the temporal lobe and hippocampus; 2: IOC of the frontal lobe; 3: IOC of the parietal lobe; 4: location and colour code of the IOC; Control (A): C57BL/6J mice; APP (B): APP/PS1 mice; APP + D (C): donepezil; APP + Gh (D): GAPT high dose; APP + Gm (E): GAPT middle dose; APP + Gs (F): GAPT small dose. The average cerebral glucose uptake rates in ROIs of the model group were lower than those of the control group, and compared with the model group, the glucose uptake average rates in the ROIs were increased in the donepezil group and GAPT middle- and small-dose groups.

from a standard curve drawn from the melting curves of the cDNA amplification products of PI3K mRNA (Figure 4(b)) and Akt mRNA (Figure 5(c)). The results showed that PI3K mRNA and Akt mRNA were highly expressed in the normal group compared with the model group ($P < 0.05$). Expression of PI3K mRNA was increased in the donepezil group and GAPT middle-dose group. The expression of Akt mRNA was increased in the donepezil group, while that of the GAPT groups tended to increase; however, there was no statistical significance.

Effects of GAPT on GLUT1 and GLUT3 expression levels on APP/PS1 transgenic mice. Immunohistochemical staining showed positive brownish-yellow coloured cell membranes in the hippocampal CA1 region of APP/PS1 transgenic mice. The expression of

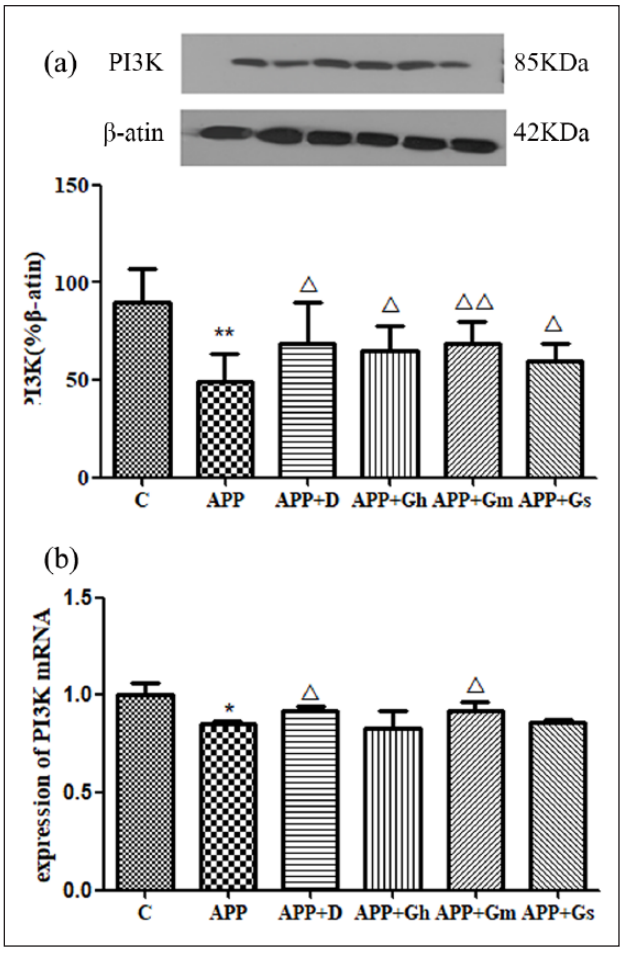

Figure 4. (a) Expression of PI3K in the hippocampus of APP/PS1 transgenic mice was determined by western blotting. (b) Expression of PI3K mRNA was determined by RT-PCR. Control: C57BL/6J mice; APP: APP/PS1 mice; APP + D: donepezil; APP + Gs: GAPT small dose; APP + Gm: GAPT middle dose; APP + Gh: GAPT high dose. *$P < 0.05$ versus control group, **$P < 0.01$ versus control group, △$P < 0.05$ versus model group, △△$P < 0.01$ versus model group; ANOVA. The PI3K expression in the donepezil- and GAPT-treated groups were all increased ($P < 0.05$), and there was significant difference between the GAPT middle-dose group and the model group ($P < 0.01$). The PI3K mRNA expression of the donepezil group and GAPT middle-dose group were increased ($P < 0.05$).

GLUT1 in the hippocampal CA1 region in APP/PS1 transgenic mice was significantly decreased compared with that of the control group ($P < 0.01$). Compared with the model group, the positive cells for GLUT1 in each treatment group were significantly increased ($P < 0.01$; Figure 7(a)). Western blot analysis showed there was a similar expression pattern for GLUT1 in each group as in the immunohistochemistry analysis (Figure 7(b)). The expression of GLUT3 in the hippocampal CA1 region in APP/PS1 transgenic mice was significantly decreased compared with that of the control group ($P < 0.01$). Compared with model group, the positive cells for GLUT3 in the donepezil group and GAPT middle-dose group were significantly increased ($P < 0.01$; Figure 7(c)).

Discussion

AD is characterized by a progressive cognitive decline along with the loss of synapses and neurons. Inadequate glucose metabolism associated with insulin/IGF resistance and deficient energy utilization was also observed in the progression of AD. APP/PS1 transgenic mice carried amyloid precursor protein (APP) and presenilin 1 (PS1) mutated genes, showing AD-like pathological features and memory impairment, which were widely used to study AD and its possible treatments.[19] As previously reported,[20] in this study, we found that, compared with the C57/BL6J mice in the control group, APP/PS1 transgenic showed a deficiency of working memory and spatial learning ability in the MWM test. The MWM test showed that, compared with the model group, the APP/PS1 transgenic mice treated with patent TCM compound GAPT had obviously shortened latencies and swimming distances ($P < 0.05$) from the third day. The target quadrant dwelling time of each GAPT treatment group was extended compared with the model group ($P < 0.05$), and the number of crossing platforms of the GAPT middle- and small-dose groups were increased ($P < 0.05$). MWM results showed that GAPT could improve the spatial learning and memory ability of APP/PS1 mice. In the SDPA test, the number of errors was reduced in the GAPT middle- and small-dose groups ($P < 0.05$ or $P < 0.01$) compared with the model group, and the latency of each GAPT group was extended ($P < 0.01$ or $P < 0.05$). These results indicated that GAPT could improve spatial learning and memory disorders in the APP/PS1 transgenic mice.

Early cognitive deficits in AD are often associated with changes in AD brain metabolism.[21] Studies have shown that the cerebral glucose metabolism in AD patients gradually decreases in specific brain regions before clinical symptoms are manifested, especially in the parietal lobe, forehead and posterior cingulate cortex.[8] Abnormal glucose levels and impaired energy metabolism result in reduced glucose utilization, thereby activating unfolded protein responses,

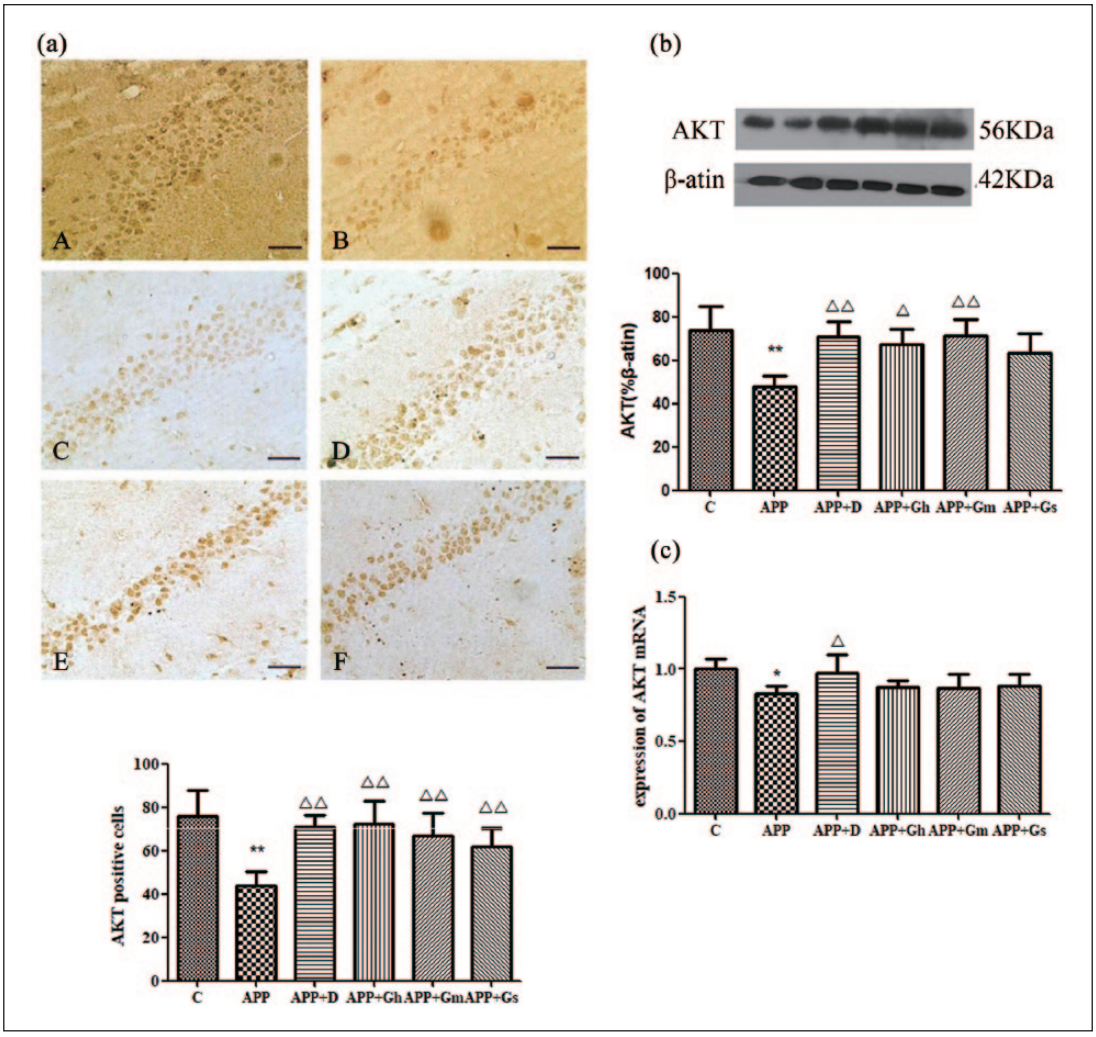

Figure 5. Expression of AKT in the hippocampus of APP/PS1 transgenic mice was determined by (a) immunohistochemistry staining and (b) western blotting. (c) Expression of AKT mRNA was determined by RT-PCR. Control (A): C57BL/6J mice; APP (B): APP/PS1 mice; APP + D (C): donepezil; APP + Gh (D): GAPT high dose; APP + Gm (E): GAPT middle dose; APP + Gs (F): GAPT small dose. *$P < 0.05$ versus control group, **$P < 0.01$ versus control group, △$P < 0.05$ versus model group, △△$P < 0.01$ versus model group; ANOVA. The expression of Akt in the hippocampus of APP/PS1 transgenic mice was significantly reduced compared with that of the control group ($P < 0.01$). Compared with the model group, the expression of Akt was significantly increased in each treatment group ($P < 0.05$ or $P < 0.01$). The AKT mRNA expression of the donepezil group was increased ($P < 0.05$).

increasing Aβ formation and deposition and, in extreme cases, leading to neuronal death.[22] PET provides a non-invasive method to quantify brain glucose metabolism, and 18F-FDG is the most commonly used cerebral glucose radiotracer analogue. The hippocampus was chosen to be the observation area because it has been closely related to the formation of learning and memory, and its damage is critical to the progression of AD. In addition, the hippocampus is the initial region of Aβ accumulation and neuronal damage.[23] With an increase in resolution, micro-PET was used to quantitatively measure changes in glucose metabolism in mouse brain regions.[24]

In this study, we observed the changes in glucose metabolism in specific regions of the brain of APP/PS1 transgenic mice (hippocampus, temporal lobe, parietal lobe and frontal lobe). The micro-PET image analysis showed that the 18F-FDG accumulation and uptake rate in the specific brain regions of the GAPT middle-dose, small-dose group and donepezil group were higher than those in the model group, suggesting that the 18F-FDG was improved in APP/PS1 transgenic mice after 3 months of GAPT treatment, and GAPT improved brain glucose metabolism abnormalities.

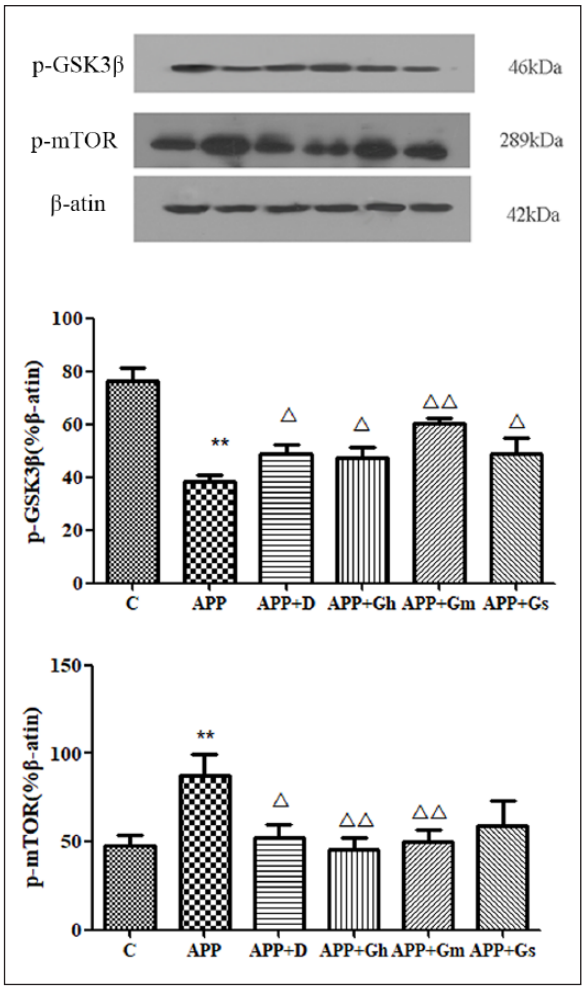

Figure 6. Expression of (a) p-GSK3β and (b) p-mTOR in the hippocampus of APP/PS1 transgenic mice was determined by western blotting. Control: C57BL/6J mice; APP: APP/PS1 mice; APP + D: donepezil; APP + Gs: GAPT small dose; APP + Gm: GAPT middle dose; APP + Gh: GAPT high dose. $^{**}P < 0.01$ versus control group, $\triangle P < 0.05$ versus model group, $\triangle\triangle P < 0.01$ versus model group; ANOVA. Compared with the model group, the expression of p-GSK3β in the donepezil group, GAPT high- and small-dose groups were increased ($P < 0.05$), while the expression of p-GSK3β in the GAPT middle-dose group was significantly increased ($P < 0.01$). The expression of p-mTOR in the donepezil group was decreased ($P < 0.05$), while the expression of p-mTOR in the GAPT high- and middle-dose groups was significantly decreased ($P < 0.01$).

In the brain, glucose was transported by the carrier protein GLUTs, which is located on the cell membrane. GLUT1 is expressed primarily in glial cells and endothelial cells, whereas GLUT3 is expressed in neurons.[25,26] It also reported that insulin can upregulate glucose transporters and increase glucose metabolism.[27] GLUT1 and GLUT3 are reduced in brain tissues of AD patients,[28] and there is a significant reduction in brain glucose metabolism and transport, as well as impaired insulin signalling. Insulin binding to the receptor causes phosphorylation of IRS and then complete activation of PI3K,[29] resulting in phosphorylation of Akt and subsequent plasma membrane transfer of GLUT and phosphorylation of GSK-3β.[30] Insulin signalling dysfunction plays an important role in the pathogenesis of AD. Studies have shown that the levels and activities of many components of the insulin PI3K-AKT signalling pathway are reduced and negatively correlated with phosphorylation of tau.[28]

Insulin/IGF-1 binds to the corresponding receptor, triggers tyrosine phosphorylation and activates the IRS family, initiating the insulin signalling cascade. Then, IRS binds to PI3K and PIP2 is converted to PIP3.[13] Increase of PIP3 causes Akt to accumulate on the membrane. Akt has many important cellular targets, including GSK3β and mTOR.

GSK3 is a serine/threonine protein kinase involved in multiple signalling processes in cells. Elevated GSK3β activity is associated with the pathogenesis of Aβ deposition, tau phosphorylation and mitochondrial dysfunction in AD. mTOR is a component of two multiprotein complexes, mTORC1 and mTORC2, that respond to cell surface receptors of insulin, growth factors and nutrients. mTOR kinase activity is elevated in the AD brain,[31] and overexpression or inhibition of mTOR in AD model mice aggravates or alleviates AD pathology and behavioural disorders, respectively.[32] Therefore, the subsequent experiments were carried out to study GLUT 1, GLUT 3 and insulin signal transduction–related proteins and to further explore the mechanism of GAPT to improve brain glucose metabolism.

The results of this study showed that the expression of GLUT1 and GLUT3 in the hippocampi of the model group was significantly lower than that of the normal group ($P < 0.01$), which was consistent with the micro-PET result. Compared with the model group, the expression of GLUT1 and GLUT3 proteins of the GAPT group was increased or significantly increased ($P < 0.05$). This suggested that by increasing the expression of brain glucose transporters, GAPT can increase glucose uptake. Compared with the normal group, the expression of PI3K and AKT in the hippocampus of the model group was significantly decreased ($P < 0.01$). Meanwhile, the PI3K mRNA and Akt mRNA of the model group were expressed at low levels, indicating that the

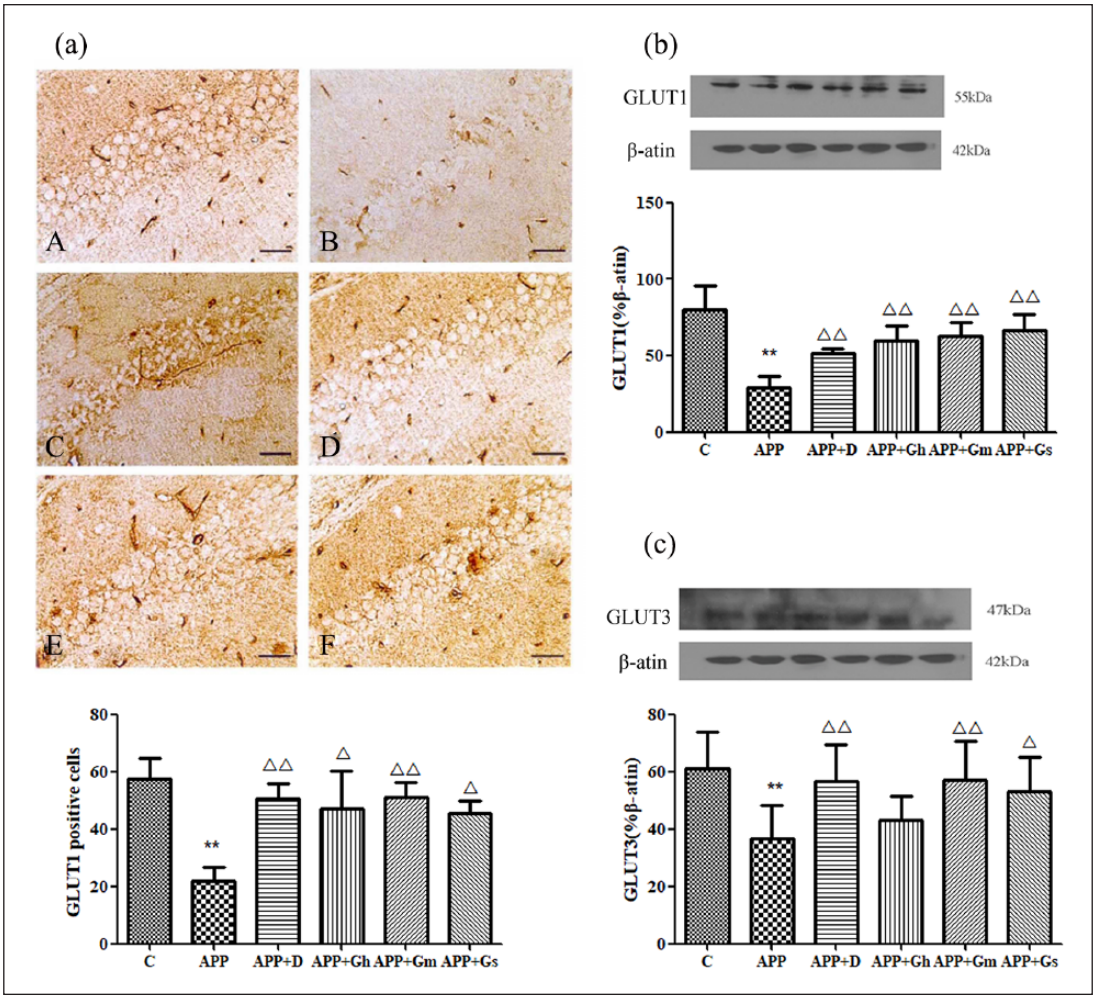

Figure 7. Expression of GLUT1 in the hippocampus of APP/PS1 transgenic mice was determined by (a) immunohistochemistry staining and (b) western blotting. (c) The expression of GLUT1 was determined by western blotting. Control (A): C57BL/6J mice; APP (B): APP/PS1 mice; APP + D (C): donepezil; APP + Gh (D): GAPT high dose; APP + Gm (E): GAPT middle dose; APP + Gs (F): GAPT small dose. $^{**}P < 0.01$ versus control group, $\triangle P < 0.05$ versus model group, $\triangle\triangle P < 0.01$ versus model group; ANOVA. The expression of GLUT1 in the donepezil group and each GAPT group were increased ($P < 0.01$). The expression of GLUT3 in the donepezil group and GAPT middle-dose group were increased ($P < 0.01$).

PI3 K/Akt pathway of APP/PS1 transgenic mice was damaged. Compared with model group mice, the expression of PI3K protein in the donepezil group and the GAPT group increased ($P < 0.05$). Immunohistochemical staining showed an increase in the number of Akt-positive cells in the GAPT group compared with the model group ($P < 0.05$). These results suggested that GAPT can increase the protein and mRNA expression of PI3 K/Akt and improve the damage of the insulin PI3K/Akt pathway. In summary, the TCM compound GAPT can improve brain glucose metabolism damage in APP/PS1 transgenic mice, mainly by increasing brain glucose uptake, increasing glucose transport and improving the insulin signalling pathway.

Declaration of conflicting interests

The author(s) declared no potential conflicts of interest with respect to the research, authorship and/or publication of this article.

Funding

The author(s) disclosed receipt of the following financial support for the research, authorship, and/or publication of this article: This study was supported by the scientific research and graduate training project of Beijing municipal commission of education (2016, 2017).

ORCID iD

Pengwen Wang https://orcid.org/0000-0003-0132-3955

References

1. Marsh J and Alifragis P (2018) Synaptic dysfunction in Alzheimer's disease: The effects of amyloid beta on synaptic vesicle dynamics as a novel target for therapeutic intervention. *Neural Regeneration Research* 13(4): 616–623.
2. Combs B, Hamel C and Kanaan NM (2016) Pathological conformations involving the amino terminus of tau occur early in Alzheimer's disease and are differentially detected by monoclonal antibodies. *Neurobiology of Disease* 94: 18–31.
3. Schaffer C, Sarad N, DeCrumpe A, et al. (2015) Biomarkers in the diagnosis and prognosis of Alzheimer's disease. *Journal of Laboratory Automation* 20(5): 589–600.
4. de Leon MJ, George AE, Ferris SH, et al. (1983) Regional correlation of PET and CT in senile dementia of the Alzheimer type. *American Journal of Neuroradiology* 4(3): 553–556.
5. Robinson RA, Amin B and Guest PC (2017) Multiplexing biomarker methods, proteomics and considerations for Alzheimer's disease. *Advances in Experimental Medicine and Biology* 974: 21–48.
6. Waldron AM, Wintmolders C, Bottelbergs A, et al. (2015) In vivo molecular neuroimaging of glucose utilization and its association with fibrillar amyloid-β load in aged APPPS1-21 mice. *Alzheimer's Research & Therapy* 7(1): 76.
7. Huang CC, Chung CM, Leu HB, et al. (2014) Diabetes mellitus and the risk of Alzheimer's disease: A nationwide population-based study. *PLoS ONE* 9(1): e87095.
8. Mosconi L, Mistur R, Switalski R, et al. (2009) FDG-PET changes in brain glucose metabolism from normal cognition to pathologically verified Alzheimer's disease. *European Journal of Nuclear Medicine and Molecular Imaging* 36(5): 811–822.
9. Szablewski L (2017) Glucose transporters in brain: In health and in Alzheimer's disease. *Journal of Alzheimer's Disease: JAD* 55(4): 1307–1320.
10. Patching SG (2017) Glucose transporters at the blood-brain barrier: Function, regulation and gateways for drug delivery. *Molecular Neurobiology* 54(2): 1046–1077.
11. Samuraki M, Matsunari I, Chen WP, et al. (2007) Partial volume effect-corrected FDG PET and grey matter volume loss in patients with mild Alzheimer's disease. *European Journal of Nuclear Medicine and Molecular Imaging* 34(10): 1658–1669.
12. de la Monte SM and Tong M (2014) Brain metabolic dysfunction at the core of Alzheimer's disease. *Biochemical Pharmacology* 88(4): 548–559.
13. O'Neill C (2013) PI3-kinase/Akt/mTOR signaling: Impaired on/off switches in aging, cognitive decline and Alzheimer's disease. *Experimental Gerontology* 48(7): 647–653.
14. Shi L, Zhang Z, Li L, et al. (2017) A novel dual GLP-1/GIP receptor agonist alleviates cognitive decline by re-sensitizing insulin signaling in the Alzheimer icv. *Behavioural Brain Research* 327: 65–74.
15. Shi J, Tian J, Zhang X, et al. (2012) A combination extract of ginseng, epimedium, polygala, and tuber curcumae increases synaptophysin expression in APPV717I transgenic mice. *Chinese Medicine* 7(1): 13.
16. Shi J, Tian J, Zhang X, et al. (2013) A combination extract of Renshen (Panax Ginseng), Yinyanghuo (Herba Epimedii Brevicornus), Yuanzhi (Radix Palygalae) and Jianghuang (Rhizoma Curcumae Longae) decreases glycogen synthase kinase 3beta expression in brain cortex of APPV7171 transgenic mice. *Journal of Traditional Chinese Medicine = Chung I Tsa Chih Ying Wen Pan* 33(2): 211–217.
17. He YK, Wang PW, Wei P, et al. (2016) Effects of curcumin on synapses in APPswe/PS1dE9 mice. *International Journal of Immunopathology and Pharmacology* 29(2): 217–225.
18. Wang PW, Su C, Feng HL, et al. (2017) Curcumin regulates insulin pathways and glucose metabolism in the brains of APPswe/PS1dE9 mice. *International Journal of Immunopathology and Pharmacology* 30(1): 25–43.
19. Li X, Bao X and Wang R (2016) Experimental models of Alzheimer's disease for deciphering the pathogenesis and therapeutic screening (Review). *International Journal of Molecular Medicine* 37(2): 271–283.
20. Ding Y, Qiao A, Wang Z, et al. (2008) Retinoic acid attenuates beta-amyloid deposition and rescues memory deficits in an Alzheimer's disease transgenic mouse model. *The Journal of Neuroscience* 28(45): 11622–11634.
21. Herholz K (2010) Cerebral glucose metabolism in preclinical and prodromal Alzheimer's disease. *Expert Review of Neurotherapeutics* 10(11): 1667–1673.
22. Chung J, Yoo K, Kim E, et al. (2016) Glucose metabolic brain networks in early-onset vs. late-onset Alzheimer's disease. *Frontiers in Aging Neuroscience* 8: 159.
23. Murray ME, Przybelski SA, Lesnick TG, et al. (2014) Early Alzheimer's disease neuropathology detected by proton MR spectroscopy. *The Journal of Neuroscience* 34(49): 16247–16255.
24. Shokouhi S, Claassen D, Kang H, et al. (2013) Longitudinal progression of cognitive decline correlates with changes in the spatial pattern of brain 18F-FDG PET. *Journal of Nuclear Medicine* 54(9): 1564–1569.
25. Dick AP, Harik SI, Klip A, et al. (1984) Identification and characterization of the glucose transporter of

the blood-brain barrier by cytochalasin B binding and immunological reactivity. *Proceedings of the National Academy of Sciences of the United States of America* 81(22): 7233–7237.
26. McCall AL, Van Bueren AM, Moholt-Siebert M, et al. (1994) Immunohistochemical localization of the neuron-specific glucose transporter (GLUT3) to neuropil in adult rat brain. *Brain Research* 659(1–2): 292–297.
27. Uemura E and Greenlee HW (2006) Insulin regulates neuronal glucose uptake by promoting translocation of glucose transporter GLUT3. *Experimental Neurology* 198(1): 48–53.
28. Liu Y, Liu F, Iqbal K, et al. (2008) Decreased glucose transporters correlate to abnormal hyperphosphorylation of tau in Alzheimer disease. *FEBS Letters* 582(2): 359–364.
29. Esposito DL, Li Y, Vanni C, et al. (2003) A novel T608R missense mutation in insulin receptor substrate-1 identified in a subject with type 2 diabetes impairs metabolic insulin signaling. *The Journal of Clinical Endocrinology and Metabolism* 88(4): 1468–1475.
30. Khan AH and Pessin JE (2002) Insulin regulation of glucose uptake: A complex interplay of intracellular signalling pathways. *Diabetologia* 45(11): 1475–1483.
31. Perluigi M, Di Domenico F and Butterfield DA (2015) mTOR signaling in aging and neurodegeneration: At the crossroad between metabolism dysfunction and impairment of autophagy. *Neurobiology of Disease* 84: 39–49.
32. Caccamo A, Magri A, Medina DX, et al. (2013) mTOR regulates tau phosphorylation and degradation: Implications for Alzheimer's disease and other tauopathies. *Aging Cell* 12(3): 370–380.